ELSEVIER

Journal of Hydrology 255 (2002) 169–193

Journal of Hydrology

www.elsevier.com/locate/jhydrol

Comparison of land surface hydrology in regional climate simulations of the Baltic Sea catchment

B.J.J.M. van den Hurk[a,*], L.P. Graham[b], P. Viterbo[c]

[a]*Royal Netherlands Meteorological Institute, P.O. Box 201, 3730 AE De Bilt, The Netherlands*
[b]*Rossby Centre, Swedish Meteorological and Hydrological Institute, SE-60176 Norrköping, Sweden*
[c]*European Centre for Medium-Range Weather Forecasting, Reading, UK*

Received 23 June 2000; revised 1 August 2001; accepted 7 September 2001

Abstract

Simulations with a regional climate model RACMO were carried out over the catchment area of the Baltic Sea for the growing season 1995. Two different surface schemes were included which in particular differed with respect to the parameterization of runoff. In the first scheme (taken from ECHAM4), runoff is a function of the subgrid distribution of the soil moisture saturation. In the second model (taken from ECMWF), runoff is a result of deep-water drainage. A large-scale hydrological model of the catchment, HBV-Baltic, was calibrated to river discharge data and forced with observed precipitation, yielding independent comparison material of runoff of the two RACMO simulations.

The simulations showed that the temporal and spatial simulation of precipitation in the area is sensitive to the choice of the land surface scheme in RACMO. This supported the motivation of analysing the land surface hydrological budgets in a coupled mode.

The comparison of RACMO with HBV-Baltic revealed that the frequency distribution of runoff in the ECMWF scheme shows very little runoff variability at high frequencies, while in ECHAM4 and HBV the snow melt and (liquid) precipitation are followed by fast responding runoff events.

The seasonal cycle of soil water depletion and surface evaporation was evaluated by comparison of model scores with respect to relative humidity. Results suggest that the surface evaporation in the ECMWF scheme is too strong in late spring and early summer, giving rise to too much drying later in the season.

Keywords: Runoff; Hydrological cycle; Land surface; Limited area climate modelling

1. Introduction

Simulation of weather events or global climate in numerical weather prediction (NWP) or general circulation models (GCMs) involves the treatment of the water distribution at the land surface. This treatment is performed by a wide variety of land surface parameterization (LSP) schemes embedded in these numerical models. Many LSP schemes have been developed in the past decades, both from the large scale NWP or GCM atmospheric point of view (e.g. Dickinson et al., 1993; Viterbo and Beljaars, 1995) and from a hydrological perspective (Dümenil and Todini, 1992; Lindström et al., 1997). A significant number of studies are dedicated to the evaluation of these LSP-schemes using observations at point, regional or global scale. The approach of these evaluation studies ranges from off-line model simulations using driving atmospheric forcings at a reference level close to the surface to fully coupled land surface — atmospheric

* Corresponding author.

0022-1694/02/$ - see front matter
PII: S0022-1694(01)00518-2

circulation models. These studies reveal significant impact of land surface processes on the hydrological cycle. Simultaneously, many models are shown to have severe difficulties in accurate simulations of evaporation, runoff and soil moisture evolution.

This paper addresses the performance of two LSP-schemes for calculating land surface hydrological budget terms on the scale of the entire catchment of the Baltic Sea, where runoff plays a major role in the surface hydrological balance. We have selected two LSP-schemes which are considered to represent two rather different approaches to the parameterization of surface runoff. In the LSP-scheme of the European Centre for Medium-range Weather Forecasts (ECMWF) (Viterbo and Beljaars, 1995), runoff is dominated by slow deep drainage. In contrast, rapid surface runoff resulting from a variable infiltration capacity scheme is the major contribution to total runoff in the ECHAM4 LSP-scheme (Dümenil and Todini, 1992). In addition, soil hydrological characteristics affecting the soil water stress on canopy transpiration are different in these models. Differences with respect to the formulation of vegetation, roughness and surface radiative properties have been removed as much as possible, to enable a focus on the soil hydrological parameterization. The schemes are implemented in a common Regional Atmospheric Climate MOdel RACMO (Christensen et al., 1996), forced by NWP atmospheric analyses at the lateral boundaries. Calculations were carried out for a single growing season between 1 March and 1 November 1995, and the analysis focuses both on the seasonal hydrological budget of the land area in the Baltic Sea catchment and on the time scales of runoff generation.

Where possible, direct observations of river discharge are the preferred validation material for runoff (Lau et al., 1996). In the Baltic Basin, these are highly affected by both extensive hydropower regulation in the Scandinavian Mountains in Sweden and by numerous large lakes in other parts of the basin. To compare LSP generated runoff, a calibrated river routing scheme could be used to include these effects by producing equivalent river discharge at river mouths from model output (Liston et al., 1994; Hagemann and Dümenil, 1999). However, such a scheme is currently not available for this region. An alternative is to use a calibrated hydrological model that can trace the river discharge signal back to runoff generation equivalent to that produced by LSP schemes.

The HBV-Baltic hydrological model (Graham, 1999) is calibrated and validated to observed discharge from 25 large subbasins covering the Baltic Sea catchment over the period 1981–1991. Using synoptic observations as input, it has been applied operationally to estimate total runoff to the Baltic Sea after 1991. For the simulation period presented in this paper, runoff generation prior to river routing is extracted from HBV-Baltic for comparison to runoff in the LSP schemes. Although results from HBV-Baltic are a step removed from true observations, they are the best available estimate of the large-scale runoff generation to the Baltic Sea.

A brief review of papers addressing the evaluation of land surface hydrology models is presented in Section 2, and subsequently a description of the procedure followed in this study is given in Section 3. In Section 4, we analyse the impact of the different LSP-schemes on the precipitation generated by RACMO. A clear change of the total precipitation and its frequency distribution is shown, indicating that the impact of the LSP treatment is beyond the surface hydrology alone. We further address this LSP-impact in the coupled simulations, and analyse the seasonal hydrological budget of the land area in the Baltic Sea catchment. We also focus on the time scales of runoff in the different schemes, and analyse the results for both a flat and a mountainous subbasin in the Baltic Sea catchment.

2. Evaluation studies addressing land hydrology in large scale models

To represent correctly the surface hydrological budget, the fundamental tasks of LSP-schemes can be identified as (a) representation of the time scales involved with the accumulation of precipitation as snow (for high latitude hydrology), (b) division of precipitation (and snow melt) over runoff and storage in the unsaturated zone, and (c) representation of the amount of soil water that is returned to the atmosphere by means of bare soil evaporation and canopy transpiration. Here, runoff is defined as the water that is not absorbed in the soil's unsaturated zone (Wetzel et al., 1996). In large-scale atmospheric models, it is

usually treated as a water sink, to be considered as a return water flow from the land area into the oceans.

Where precipitation is usually treated as a given forcing to the land surface scheme, land–atmosphere feedbacks result in modifications to the precipitation simulations as a result of changes in the land surface treatment solely (see e.g. the review of Pitman et al., 1999). Evaluation of land surface processes using off-line (intercomparison) experiments do not address this feedback. The design of the Project for Intercomparison of Land-surface Parameterization Schemes (PILPS) (Henderson-Sellers et al., 1993) fully acknowledges this by organizing experiments ranging from off-line single column model runs to fully coupled GCM simulations.

Comparing off-line surface schemes has been used to demonstrate the direct effects of the land hydrology parameterization on runoff and evaporation. Studies have been carried out using observed forcings at a single location (e.g. Shao et al., 1994) or at a continental scale (Wood et al., 1998). Results from these studies showed that the accuracy of simulations of drainage and runoff is very poor in most schemes, and runoff is considerably underpredicted when forced with near surface observations (Shao et al., 1994; Wetzel et al., 1996; Dirmeyer and Dolman, 1998). Parameterization of runoff is shown to have a large effect on the runoff variability at seasonal time scales and shorter, and on the seasonal cycle of surface evaporation which is significantly affected by the runoff treatment (Lohmann et al., 1998). Koster and Milly (1997) pointed at the importance of the relationship *between* evaporation reduction *and* runoff generation for the hydrological balance in an LSP, rather than by the formulation of these processes separately. Obviously, simulations of evaporation are affected by the runoff parameterization scheme (and vice versa), and these schemes should be compatible.

Also, evaluation of coupled land-atmosphere models has been carried out in a number of studies. Lau et al. (1996) analysed the hydrological cycle of GCM-simulations during the first Atmospheric Model Intercomparison Project (AMIP) (Gates, 1992) experiment. One of the evaluations carried out was an intercomparison of GCM runoff output passed through a river-routing model to actual hydrographic data from river runoff from the Mississippi and the Amazon basins. They found that the ensemble mean runoff ($=$ precipitation $-$ evaporation) from the participating GCMs matched the observations reasonably well, but the spread among the models covered more than an order of magnitude. A major part of the differences between the models was caused by differences in precipitation, but the differences in runoff seasonality displayed in the AMIP intercomparison point at a clear role of the land surface component. They conclude that the use of climate models for basin-scale hydrological purposes is still highly questionable. Robock et al. (1998) point at the potential importance of feedback processes in the hydrological cycle connecting land evaporation, precipitation and runoff, which may cause year-to-year variability of soil moisture content only poorly captured by the GCMs joining the AMIP experiment.

In the context of another continental scale experiment, the Baltic Sea Experiment (BALTEX), Graham and Jacob (2000) compared simulated runoff for a 10 year period (based on sea surface temperatures for 1979–1988) from the ECHAM4 global climate model with output from the calibrated semi-distributed hydrological model HBV-Baltic (Graham, 1999), forced with both observed precipitation and ECHAM4 calculated precipitation. Also in the latter comparison set-up, large seasonal differences were present between direct ECHAM4 output and HBV-Baltic results. In particular during the spring and summer seasons, ECHAM4 generates much lower runoff, feeding back to large differences in the seasonal cycle of soil water storage.

In these studies, global circulation models were used to generate the forcing to the land surface parameterization schemes. Although use of observed sea surface temperatures (SST) puts a climatological constraint on the model evolution, comparison to actual weather cannot be carried out in this set-up. As an alternative, in some studies use is made of the hydrological budget from reanalysis cycles from global weather prediction systems. A few papers devoted to the evaluation of the hydrological cycle in the ECMWF reanalysis (Gibson et al., 1997) revealed that runoff was underestimated by 50% in the Mississippi basin, and did not realistically respond to (heavy) precipitation events (Betts et al., 1998, 1999). Part of the deficiency is probably caused by a spin-up problem in the reanalysis precipitation, which was compensated by soil moisture adjustments

derived from atmospheric humidity biases (Viterbo and Courtier, 1995). The interplay between precipitation, soil moisture, runoff and evaporation is therefore incorrectly represented in this reanalysis, and similarly in the reanalysis cycle of NCEP (Hagemann and Dümenil, 2001).

At higher latitudes, Betts and Viterbo (2000) examined the surface energy and water balance of the Mackenzie River basin, focusing on two years of ECMWF operational forecasts. Although the annual model runoff for the whole basin was close to observed streamflow, the spring runoff peak occurred a month too early. Additionally, errors in the spatial distribution of runoff were associated with large values of the soil moisture adjustments, trying to compensate for deficiencies in the runoff formulation.

It is unclear how the repeated update of atmospheric fields in the analysis procedure affects the hydrological feedback between the surface and the atmosphere. Therefore, an intermediate procedure is to use coupled limited area models, which evolve freely within the model domain, but pick up actual weather patterns from analyses used as lateral forcing (e.g. Giorgi et al., 1993; Christensen et al., 1996; Jacob and Podzun, 1997). Jacob et al. (2001) compared a set of eight standardized regional atmospheric models during the simulation of a 3-month summer/autumn period in the Baltic Sea area. The soil water content in the models was not brought into an equilibrium state before starting the comparison runs, which gave rise to large differences in land surface evaporation as a response to different initial soil moisture conditions. Also, large differences in the simulated surface runoff (compared to a HBV-Baltic series) were present. Many interacting processes in the models made a firm conclusion on the performance of the individual land surface parameterization schemes rather difficult.

A correct representation of runoff in a GCM will obviously include both a good estimate of the fraction of precipitation that eventually leads to runoff production, and a proper representation of the frequency distribution of runoff events. Total runoff estimates on a seasonal or year-to-year basis are relevant for the assessment of the amount of water available for evapotranspiration, which both feeds the hydrological cycle and puts a constraint on vegetation growth. Frequency distributions are relevant to forecasting of extreme flooding events, and planning of hydropower and dam releases. Given the importance of land surface runoff in the general hydrological balance and parameterization of evaporation, and given the spread of the various LSP and GCMs used nowadays, a further evaluation of the runoff treatments in large scale atmospheric models is desirable.

3. Description of the models and simulation strategy

3.1. Runoff in large scale models

We can identify two different general approaches in the surface runoff treatment in land surface schemes. In the first approach, surface runoff only occurs when the potential water inflow (precipitation + snow melt − interception loss) exceeds the maximum infiltration rate of a (shallow) upper soil layer. The surface scheme in the ECMWF GCM (Viterbo and Beljaars, 1995) is designed in this way. However, as the upper soil layer in this scheme is relatively deep, and the water flow to lower layers is efficient, saturation of the upper layer and thus exceedance of the infiltration capacity is never simulated. Virtually, all runoff generated in the ECMWF-surface scheme is a result of drainage flow from the lowest soil layer. Other examples of schemes with a small or negligible surface runoff production are CHASM (Desborough, 1999) and CLASS (Verseghy, 2000). In a second approach of surface schemes, surface runoff is produced at a rate proportional to a specified relative saturation in the GCM grid box. This implies that the soil is assumed to be saturated in part of the grid box, and additional water inflow in this part of the grid box will be treated as runoff. The area covered with saturated soil is parameterized as a function of the average soil moisture content in the grid box, and a topographic correction, resulting in a higher saturation degree in mountainous areas. As an example, the surface scheme in the ECHAM4 climate model (Dümenil and Todini, 1992) is constructed in this way. Other examples are VIC (Liang et al., 1996) and newer versions of ISBA (Noilhan and Mahfouf, 1996).

The response time scales of the surface runoff and the deep-water drainage are different. Surface runoff is generated instantaneously when precipitation or

Table 1
Summary of average initial values and land surface parameters for all gridpoints in the Baltic Sea Catchment subarea

Parameter	Units	ECHAM4	ECMWF
Geopotential height	m^2/s^2	1761	1761
Leaf area index	m^2/m^2	3.26	3.26
Vegetation coverage	–	0.59	0.59
Forest coverage	–	0.48	0.48
Maximum soil water content	m	0.295	–
Orographic standard deviation	m	52	–
Initial snow depth	mm (water equiv.)	56.9	56.9

melting snow cannot be absorbed quickly in the soil layer close to the surface. Deep-water drainage, on the other hand, has a much slower response (similar to water storage in lakes). Moreover, the soil volume in between may act as a time filter, depending on the storage capacity of the soil and the processes acting on the water travelling through it (root extraction, gravity drainage, freezing).

3.2. The ECHAM4 land surface scheme

In the hydrological component of the ECHAM4 land surface scheme (Dümenil and Todini, 1992), a single soil moisture reservoir is filled by precipitation and snow melt, and depleted by extraction from plant roots, bare soil evaporation and deep water drainage. The net water flux to the soil, the throughfall T, is governed by rainfall, snow melt and interception by plants (see Appendices A and B). Precipitation falling as snow is stored in the snow deck, and thus does not contribute to throughfall until it melts.

When at a given location in the grid box the soil moisture content has reached saturation, surface runoff R_s is assumed to occur. The fraction of the grid box that is saturated, S, is a parameterized function of the average soil moisture content in the grid box W, the saturation soil moisture content W_{sat}, and the orographic standard deviation σ_o. S is given by:

$$S = 1 - \left(1 - \frac{W}{W_{sat}}\right)^b. \tag{1}$$

The coefficient b is a grid box dependent parameter, expressed as a function of σ_o according to:

$$b = 0.01 \leq \frac{\sigma_o - \sigma_{min}}{\sigma_o + \sigma_{max}} \leq 0.5, \tag{2}$$

with σ_{min} and σ_{max} kept constant at 100 and 1000 m, respectively. All throughfall exceeding the saturation limit is removed as surface runoff. Integrating Eq. (1) over the grid box area results in (Dümenil and Todini, 1992)

$$R_s = T - (W_{sat} - W) + W_{sat}\left[\left(1 - \frac{W}{W_{sat}}\right)^{1/(b+1)} - \left(\frac{T}{(b+1)W_{sat}}\right)\right]^{b+1}. \tag{3}$$

Eqs. (1)–(3) result in efficient surface runoff for grid boxes where either W/W_{sat} or σ_o is large. In the implementation of the scheme in this study, W_{sat} varies over the domain, following Claussen et al. (1994). σ_o is derived from the variance of the topographic height.

A deep drainage term, R_D, is added to the runoff to account for the slow process of water loss to ground water tables and organized stream flows. Dümenil and Todini (1992) formulate R_D as

$$R_D = \begin{cases} D_{min}\dfrac{W}{W_{sat}} & W < W_D \\ D_{min}\dfrac{W}{W_{sat}} + (D_{max} - D_{min})\left(\dfrac{W - W_D}{W_{sat} - W_D}\right)^c & W \geq W_D \end{cases} \tag{4}$$

with D_{min} and D_{max} the minimum (10^{-3} mm/h) and maximum (10^{-1} mm/h) drainage rates, respectively, W_D a fast drainage threshold (90% of W_{max}), and $c = 1.5$.

The canopy transpiration is regulated using a canopy resistance depending on environmental conditions including soil moisture content (see Appendices A and B). It linearly responds to the soil moisture

Table 2
Soil physical coefficients in the ECMWF surface scheme

Parameter	Units	Value
γ_{sat}	m/s	4.57×10^{-6}
Ψ_{sat}	m	−0.346
b_c	–	6.0
w_{sat}	m^3/m^3	0.472
w_{cap}	m^3/m^3	0.323
w_{pwp}	m^3/m^3	0.171
Layer depth 1	m	0.07
Layer depth 2	m	0.21
Layer depth 3	m	0.72
Layer depth 4	m	1.89

content in the single soil moisture reservoir between 35 and 75% of the maximum reservoir depth. With $W_{max} = 295$ mm on average for the Baltic Sea catchment area (see Table 1), the active soil moisture range is approximately 118 mm. Additional relevant parts of the ECHAM4 surface scheme are described in Appendix A.

3.3. The ECMWF land surface scheme

The ECMWF land surface scheme (Viterbo and Beljaars, 1995) has been operational since 1994 and was used in the 15-year reanalysis (1979–1993), ERA15 (Gibson et al., 1997).

The soil hydrological budget is solved by means of a simplified Richards equation applied to a vertical stack of four layers (Table 2). For each layer, the soil moisture content w is calculated using

$$\frac{\partial w}{\partial t} = -\frac{\partial}{\partial z}\left(\lambda \frac{\partial w}{\partial z} - \gamma\right) - S_w, \tag{5}$$

in which z is depth, λ is the hydraulic diffusivity, γ the hydraulic conductivity generating a downward force due to gravity, and S_w a root extraction sink term. λ and γ are based on the widely used parameterization of Clapp and Hornberger (1978):

$$\gamma = \gamma_{sat}\left(\frac{w}{w_{sat}}\right)^{2b_c+3}, \tag{6}$$

$$\lambda = \frac{b_c \gamma_{sat}(-\Psi_{sat})}{w_{sat}}\left(\frac{w}{w_{sat}}\right)^{b_c+2}. \tag{7}$$

with Ψ_{sat} the soil hydraulic pressure at saturation. The coefficients in these formulations are similar everywhere, and taken from an 'average' soil texture class (see Table 2).

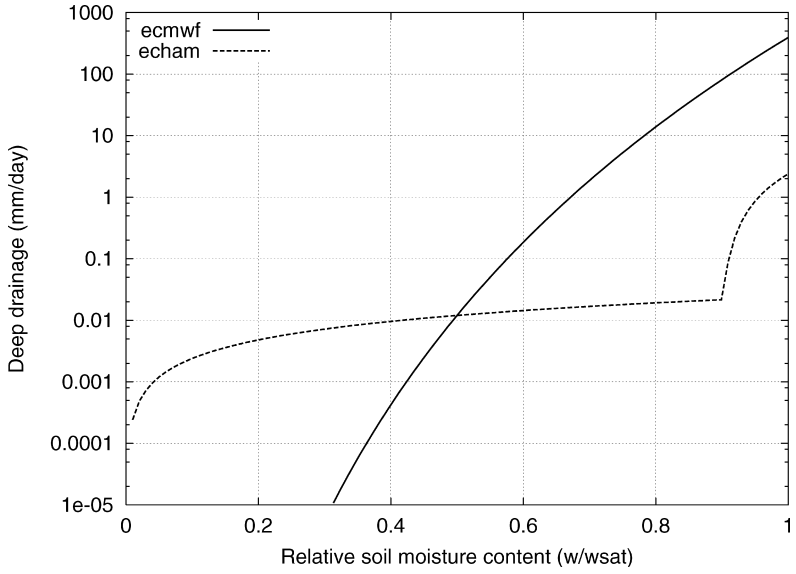

Fig. 1. Deep drainage rate in the ECHAM4 scheme, given by Eq. (4), and in the ECMWF scheme, from Eq. (6), expressed as function of the relative soil saturation.

The generation of runoff is a result of either of the following processes:

Surface runoff is produced when the throughfall rate T exceeds the maximum infiltration capacity, which is given by

$$\rho_w\left(\frac{b_c\gamma_{sat}(-\Psi_{sat})}{w_{sat}}\frac{w_{sat}-w_1}{0.5z_1}+\gamma_{sat}\right), \quad (8)$$

with w_1 and z_1 the water content and depth of the upper layer, respectively. For a soil with the upper layer at field capacity ($w_1 = 0.323\ m^3/m^3$), this requires a throughfall rate of >300 mm/h, so in practice this condition is never met.

Deep runoff is given by the free drainage rate from the lowest soil layer, Eq. (6). Drainage always occurs, rather than being episodic as in ECHAM4 and HBV-Baltic. This is the major runoff contribution.

Saturation runoff occurs when any of the four layers becomes supersaturated: additional water is removed as runoff. This is also a runoff mechanism which in practice never occurs.

While surface runoff in the ECMWF scheme is an inefficient mechanism to remove water from the soil, the deep-water drainage is effective in a wide range of w/w_{sat}. A comparison of γ (Eq. (6)) to the drainage component in the ECHAM4 runoff (Eq. (4)) is shown in Fig. 1. γ varies by many orders of magnitude, but drainage is effectively negligible when $w/w_{sat} < 0.5$. In the ECHAM4 scheme, a slow drainage rate is always present. Under (moderately) wet conditions, the ECMWF drainage always exceeds the ECHAM4 rate. ECHAM4 loses significant amounts of water via drainage only at near-saturation conditions.

The response of canopy transpiration to environmental conditions is similar to the ECHAM4 treatment, although the different structure of the soil imposes differences in the soil water stress. The root zone water content is defined as a root weighted average of the upper three soil layers (extending to 1 m depth), where a linear dependence between 0.171 and $0.323\ m^3/m^3$ is incorporated. This implies an active range of 152 mm, which is nearly 30% larger than in ECHAM4. In order to keep remaining vegetation characteristics compatible to the ECHAM4 approach, standard ECMWF parameters for the minimum stomatal resistance $r_{s,min}$ and leaf area index were replaced by ECHAM4 values (including a variable leaf area index distribution). Appendix B gives additional details on the ECMWF surface scheme and the remaining differences to ECHAM4.

3.4. The regional atmospheric model and its initialization

Both the ECHAM4 and ECMWF surface schemes were embedded in a common host model called RACMO (Christensen et al., 1996). The dynamical package in RACMO is similar to the HIRLAM limited area weather forecast model (Gustafsson, 1993), but the physical parameterization is taken from the ECHAM4 climate model (Roeckner et al., 1996). Also the model's infrastructure for input/output, pre- and postprocessing, initialization and code organization is taken from the HIRLAM system.

The default land surface scheme is the variable saturation scheme by Dümenil and Todini (1992). A special version was prepared in which this surface scheme was replaced by the ECMWF LSP (Viterbo and Beljaars, 1995). This involved particularly the introduction of additional soil layers and the revision of the interface between the surface and the atmosphere via the extra skin layer.

For this study, RACMO is situated over the Baltic Sea area (see Fig. 2). The grid is set up with a distance of $\approx 1/6°$ (approximately $16 \times 16\ km^2$) at the equator and rotated to the domain. The total number of grid points is $122 \times 182 = 22\,204$. The vertical column is divided into 24 layers, the lowest of which is at about 30 m above the surface. Time step is 120 s.

The simulations cover the period between 1 March and 1 November 1995. In general, soil moisture content is highest in early spring, when winter precipitation and early snow melt have filled up the soil reservoir before evaporation becomes active. The period covers a complete growing season, and shows a clear signature of the behaviour of the different runoff schemes examined. Moreover, the simulation interval is guided by earlier regional model intercomparisons carried out during the PIDCAP intensive evaluation period between 1 August and 1 November 1995, executed in the context of BALTEX model activities (Jacob et al., 2001). From a hydrological perspective, the chosen timeframe is not

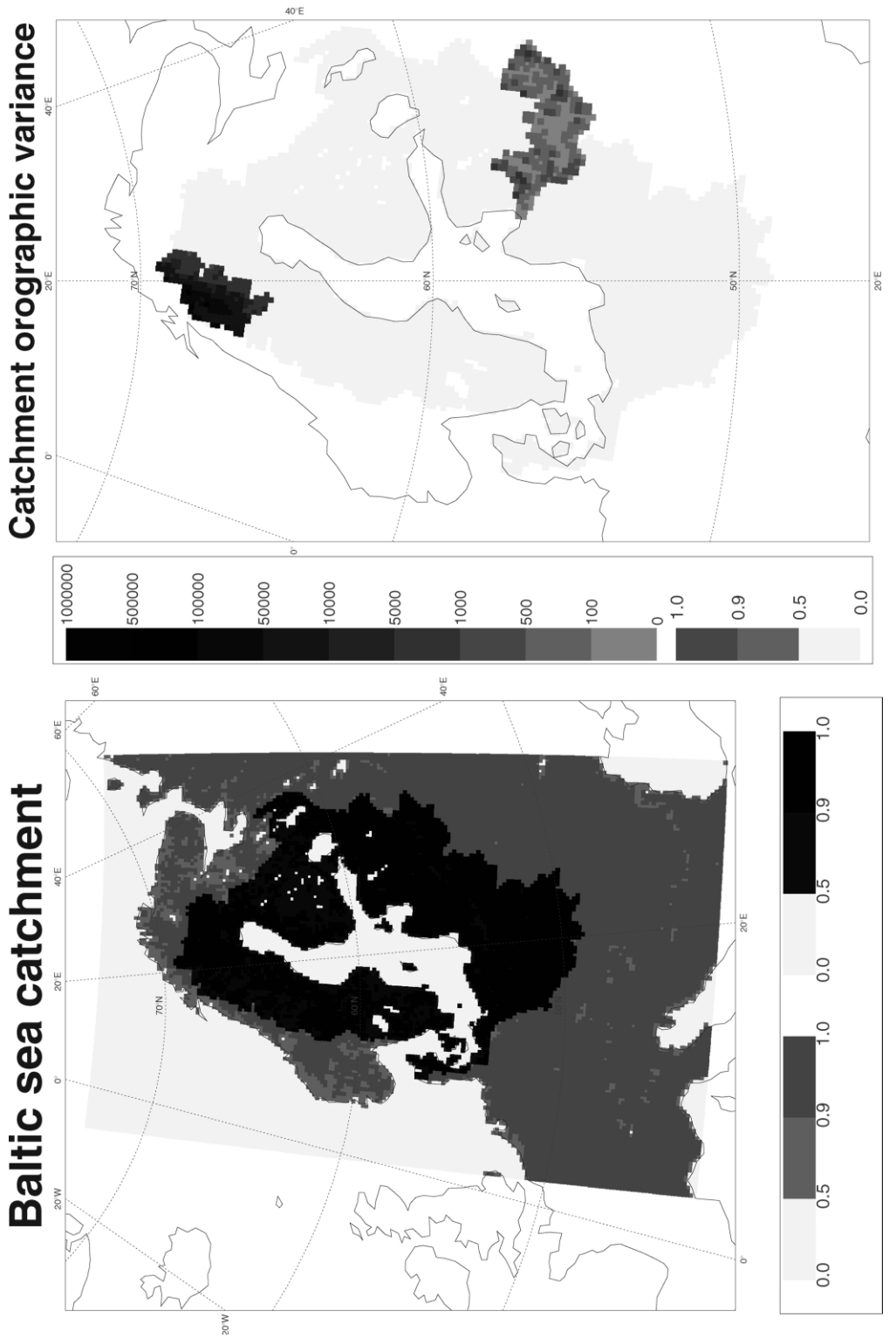

Fig. 2. Left: model domain and Baltic Sea catchment; right: geographic position of the two subcatchments Bothnian Bay (upper area) and Gulf of Riga (area in south-east), shown by the values of σ_o^2 within the catchment.

optimal, as snow accumulation over the winter 1994/1995 is not included in the regional model simulations. The snow depth climatology used for initialization of the LSP schemes does show clear differences from the HBV-Baltic simulation. Also, the choice to initialize the soil moisture content at saturation (ECHAM4) or field capacity (ECMWF) (see below) is somewhat arbitrary, and may deviate from soil moisture fields obtained from a simulation sequence initialized before the current timeframe.

Initial atmospheric fields, sea surface temperature and lateral atmospheric boundary conditions are interpolated from operational 6-hourly global analyses produced by ECMWF. Soil temperatures are initialized by propagating the climatological annual cycle of the surface temperature from the ECHAM4 global climate model into the soil using the locally defined thermal diffusivities and heat capacity. Surface parameters (leaf area index, vegetation and forest coverage, maximum soil water content in the ECHAM4 scheme, geopotential height, surface roughness, orographic variability) were interpolated from the ECHAM4 climate system (Claussen et al., 1994). The snow pack was initialized at ECHAM4 climatological values.

Since the soil moisture treatment in the models is different, its initialization is necessarily somewhat arbitrary. Here we have chosen to initialize the depth of the soil water column in the model root zone to be similar for the models involved. In the ECHAM4 scheme, soil water was therefore initialized at full saturation (on average 0.295 m), whereas ECMWF soil water was initialized at field capacity (implying 0.323 m water in the top 1 m of soil). Geographical variability and different impact on both canopy transpiration and runoff generation hamper a direct comparison of soil water levels. Table 1 summarizes initial surface values in the catchment area for both LSP schemes.

3.5. The HBV hydrological model

Utilizing currently available observations, a best estimate of runoff was provided by the calibrated HBV-Baltic model (Graham, 1999) as discussed above. This is the largest scale application of the HBV hydrological model to date. The HBV model was developed more than 25 years ago (Bergström and Forsman, 1973). It is a catchment based hydrological water balance model that distributes precipitation to snow accumulation and melt, soil moisture storage, evapotranspiration, groundwater storage, lake storage and runoff. River routing components are used to model the delay of runoff water before reaching the river discharge location. Recognizing the immense heterogeneity of soils even over small areas, HBV uses a single soil layer with a statistically distributed approach based on variability parameters for soil moisture modelling. This accounts for the fact that runoff does not occur simultaneously throughout a drainage basin, but rather increases or decreases nonlinearly according to the distribution of soil moisture in the basin. Since its original development, HBV has undergone significant changes and upgrades. More detail and sophistication has been added to many modelling routines, such as snow processes (Bergström, 1995; Lindström et al., 1997). However, the core of the model, its soil moisture routine, is little changed from the original. Its approach to soil moisture and runoff modelling has proven to be robust over a wide range of scales, including the continental scale (Bergström and Graham, 1998; Graham 1999; Graham and Bergström, 2000).

The primary horizontal unit in HBV is an irregularly shaped hydrological subbasin, which allows for spatial variability of precipitation, ease of model application and validation. Except for the shape, these are the equivalent to the grid boxes used in atmospheric models. However, within each subbasin, discretization into elevation zones and land use is carried out. This addresses the subbasin or subgrid variability. Vertically, HBV is organized as a series of boxes connected by vertical fluxes representing the main physical processes of snow and rain, evapotranspiration, soil moisture, quick runoff response, slow runoff response and lakes.

Runoff is expressed as a function of soil moisture content, model field capacity and total infiltration to the soil, according to:

$$R_{\mathrm{hbv}}/I_{\mathrm{hbv}} = (W/W_{\mathrm{fc}})^{\beta} \tag{9}$$

where R_{hbv} is the total runoff generation flowing out of the HBV soil box, and I_{hbv} is the net water flux to the soil, which consists of throughfall and snowmelt. W is soil moisture and W_{fc} is the model field capacity (maximum attainable soil moisture). β is an empirical

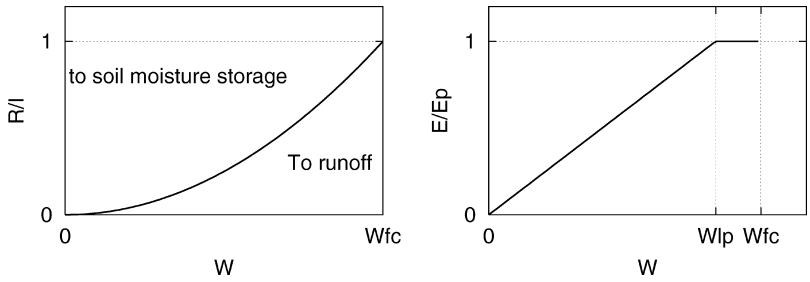

Fig. 3. HBV model components for (left) runoff generation R to increments of rain or snowmelt, I (example with $\beta = 2$), and (right) estimation of actual evapotranspiration, E from potential evaporation E_p.

constant that typically ranges between 1.5 and 4.0 (see Fig. 3). Eq. (9) is applied to each land use category for every elevation zone of all subbasins.

Evapotranspiration in the HBV model is also based on the variability of the soil moisture content. Actual evapotranspiration, E_{hbv}, is calculated as a function of potential evapotranspiration E_p. The limit for potential evapotranspiration, W_{lp}, modifies this relationship according to:

$$\frac{E_{hbv}}{E_p} = \begin{cases} W/W_{lp} & W < W_{lp} \\ 1 & W \geq W_{lp} \end{cases} \quad (10)$$

W_{lp} typically ranges between 70 and 90% of W_{fc} (Fig. 3).

Runoff generation from Eq. (9) is fed into HBVs runoff response routines, where the routing of runoff dynamics in both space and time is carried out. The upper response box represents the quick runoff response, while the lower response box represents slower runoff response processes. The total outflow from both response boxes constitutes the total river discharge from the outlet of the subbasin. This corresponds to the gauged river flows of hydrological observations.

3.6. Use of observations

Observations of total river discharge to the Baltic Sea are available for the period 1981–1991 as mean monthly values in m^3/s. For the northernmost areas, reconstructed records of natural river discharge (taking away the effects of hydropower regulation) were used. This is the best temporal resolution currently available for river discharge to the Baltic Sea. Within BALTEX, efforts are underway to collect daily river discharge data for the basin, but this has proven to be a slow process (Carlsson, 2000). Synoptic observations from some 800 stations for precipitation (12-hourly) and temperature (3-hourly) covering the period 1979–1998 from the entire Baltic Basin are available in an interpolated $1 \times 1^\circ$ grid database at the Swedish Meteorological and Hydrological Institute (SMHI) (Omstedt et al., 1997). These observations were summarized to daily values and used to drive the HBV-Baltic model. The model was run with a daily time step and calibrated against the monthly river discharge values. Using the synoptic observations, HBV-Baltic model results extend beyond the available period of the runoff record and are used as a replacement to the record until observations are available.

Fig. 4 shows results from the calibration (1981–1986) and validation (1986–1991) periods for the total Baltic Sea drainage basin and two smaller drainage basins, one from the mountainous region of the Bothnian Bay drainage basin and one from the Daugava River in the Gulf of Riga drainage basin. More information on these subbasins is given below. In addition to visual inspection, the performance of HBV-Baltic was assessed with the Nash Sutcliffe efficiency criterion, R^2 (Nash and Sutcliffe, 1970), ranging between -1 and 1 (where 1 represents a perfect fit). In addition, mass balance was maintained by minimizing the error between cumulative runoff from the model and cumulative runoff of the observations. Monthly R^2 values attained values of 0.91, 0.95 and 0.82 for the total basin, Bothnian Bay subbasin and the Gulf of Riga subbasin, respectively, for the period 1981–1991. This efficiency criterion using daily model output data and monthly averaged observations is somewhat inconsistent, but applied to the total Baltic Basin they would yield 0.83/0.84/0.83 in

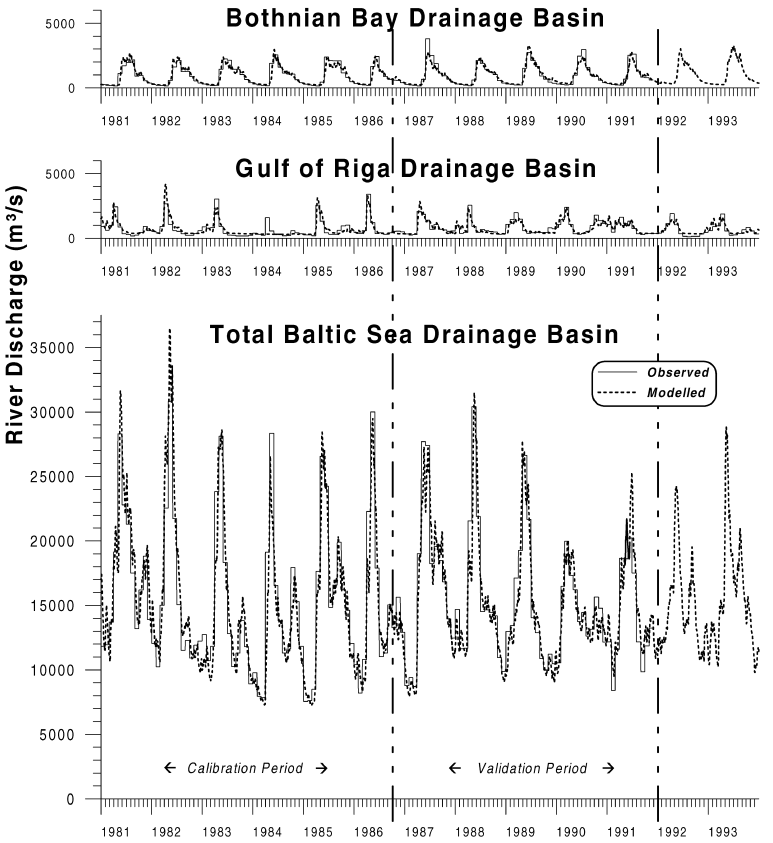

Fig. 4. Observed and modelled river discharge from HBV-Baltic for the total Baltic Sea catchment, Bothnian Bay catchment (mountains basin) and Gulf of Riga catchment (Daugava River basin).

order of calibration/validation/total. For the Bothnian Bay subbasin, scores of 0.84/0.85/0.84 are derived, whereas the skill is somewhat lower for the Gulf of Riga subbasin at 0.69/0.73/0.71. For further evaluation, Graham (1999) gives more detail on model performance.

One of the drawbacks of calibrating a daily model against monthly observations is that the resulting hydrographs tend to be somewhat smoothed as runoff peaks are dampened in the model while low flows tend to be overestimated. This is the case for the HBV-Baltic results, even though effort was made to try to keep runoff peaks above the monthly mean observations. These results are therefore most accurate when applied on monthly time scales. For the daily time scale, HBV-Baltic results are less reliable, but they are the best estimate currently available for the large-scale daily runoff. Coarser temporal scales, such as weekly and biweekly provide a more robust basis for comparison.

In the course of calibrating HBV-Baltic, corrections were applied to the synoptic precipitation observations, adding typically 10% to the measurements. This accounts for some of the aerodynamics losses in precipitation gauge measurements; although, it was not a rigorous treatment of undercatch that uses site-specific meteorological variables. Particularly, early in the season when snow fall occurs, undercatch may be underestimated. These corrected daily precipitation values were also used for direct comparison to the RACMO results.

Also available are screen level relative humidity observations at approximately 250 synops stations in the area. Relative humidity is obviously affected by many processes related to the land surface fluxes, boundary layer evolution and orographic effects.

However, it contains implicit information on both the atmospheric humidity demand and moisture condition of the underlying surface wetness, causing fairly high correlations between relative humidity and surface evaporation in model simulations. Typical values for these correlation coefficients are 0.6–0.7 for many mid-latitude daytime summer calculations. Therefore, it is considered to be a valuable indicator for surface evaporation. Relative humidity calculations for each RACMO grid box were bilinearly interpolated to the synops station locations. From these pairs of collocated observations/model results, area-averaged bias and root-mean-square (rms) values (corrected for bias) were calculated.

3.7. Postprocessing and comparison

In the following, we will consider the land surface hydrological balance of all land points in the BALTEX catchment area (see Fig. 2). RACMO output is averaged in 6 h intervals.

RACMO runoff is defined as the water that leaves the model's soil reservoir. This may be interpreted as the water that leaves the unsaturated zone in the soil. For comparison with HBV-Baltic, we use the water flow prior to the river routing scheme in this hydrological model. This is denoted as the amount of *runoff generation*. The river routing scheme in HBV-Baltic has been used for calibrating the model to river discharge data, but it is not relevant to the comparisons shown in this study.

In RACMO, a subsample of 5017 land grid-points (1 729 000 km^2) is defined, corresponding to the catchment land area of the Baltic Sea basin (see Fig. 2). This subsample was postprocessed separately, and used in most of the analyses shown later. HBV-Baltic results are calculated for 25 subbasins in the catchment area, and runoff is calculated as an area-weighted average from these subbasins.

Results from two subbasins are analysed separately (see Fig. 2): the flat Daugava River basin in the Gulf of Riga catchment (327 gridpoints; $\sigma_o \approx 0$–50 m; total area 87 900 km^2), and the mountainous headwaters of several combined Swedish rivers flowing to the Bothnian Bay (208 RACMO gridpoints; $\sigma_o \approx 30$–350 m; 47 600 km^2). The somewhat atypical representation of a hydrological catchment for the latter subbasin in HBV-Baltic is used to represent the mountainous flow regime at large scale.

In the following, the statistics and budgets will generally be calculated for the period 1 April–31 October, allowing for a one-month spin-up period. Note that, even when disregarding the entire first month of the integration, there might still be an effect of the initial conditions of soil water in the results shown.

4. Results

4.1. Precipitation time series and frequency distribution

The impact of choosing a different land surface parameterization scheme in RACMO on the calculation of total precipitation over the land area in the Baltic Sea catchment is shown in Fig. 5, where a time series of weekly averaged total precipitation over land is shown. Also shown is the precipitation derived from the corrected precipitation gauges, used to drive the HBV-Baltic model. In both set-ups, the general seasonal trend is captured, but RACMO shows an overestimation of precipitation, notably in the early and later parts of the simulation period. Simulations carried out between August and October 1995 for the same area showed a similar high precipitation bias of RACMO in September and October (Jacob et al., 2001). A similar seasonality, although less pronounced, was also found in the evaluation of ECMWF reanalysis data by Betts et al. (1998). The high bias early in the season is partially associated with an excessive sublimation of snow over snow covered forest areas, providing a great source of latent heat (Van den Hurk et al., 2001). The overestimation of precipitation in spring in the ECMWF scheme is partially compensated in the early summer period (see also below).

The bias is different for both schemes, the ECHAM4 LSP generating a stronger bias in the early months than ECMWF. This may well be associated with a difference in initial effective soil water content, affecting the surface evaporation in the snow free areas.

However, noticeable differences also occur in the frequency distribution of the precipitation intensity,

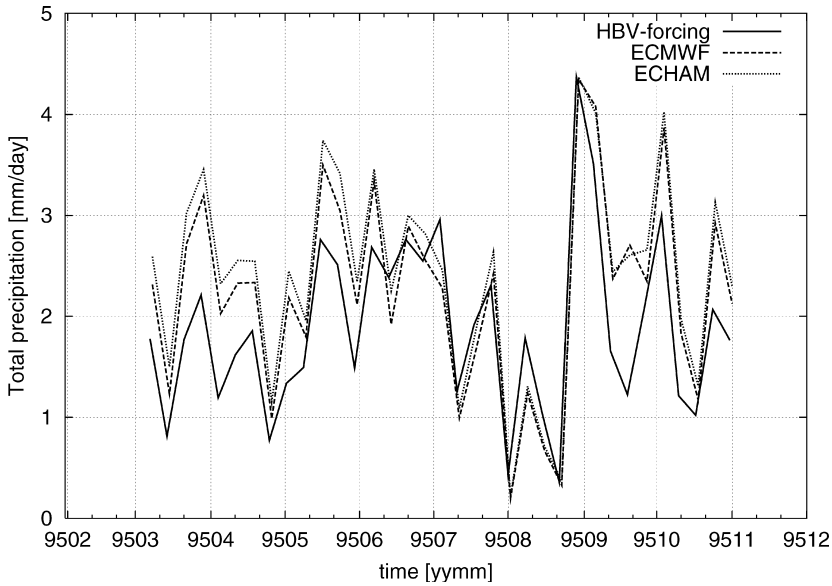

Fig. 5. Timeseries of weekly averaged total precipitation (mm/day) falling on the land area in the Baltic Sea Catchment, as derived from the interpolated rain gauges (used to force HBV), and as calculated from the RACMO atmospheric model with the ECHAM4 and ECMWF land surface schemes.

shown in Fig. 6. Shown is the frequency distribution of all RACMO gridpoints within the Baltic catchment land area with respect to the seasonally averaged total precipitation in two different periods (March–April–May and June–July–August). Where both models show a preference to generate seasonally averaged precipitation intensities of 1–2 mm/day, the ECHAM4 version has more gridpoints with intense precipitation than the ECMWF version. The shift towards more intense precipitation events in the ECHAM4 version is also displayed in the frequency distribution of catchment averaged daily precipitation (figures not shown).

Although the boundary relaxation in the limited area model imposes some control on the net precipitation in the domain, the hydrological cycle is clearly able to vary as function of the land surface parameterization. Part of this variation may be a redistribution of precipitation over the land and the sea areas in the domain. Since the differences between the ECHAM4 and ECMWF versions of RACMO are primarily determined by differences in the LSP parameterization, an off-line evaluation of these land surface schemes may conceal some of the effects of a LSP scheme on the hydrological cycle. For this reason, an evaluation in a coupled mode was carried out in this study.

4.2. Spatial and temporal variability of runoff

The basic comparison of RACMO runoff from two different surface schemes to HBV-Baltic simulated runoff for all land points in the Baltic Sea catchment area is shown in Fig. 7. This figure reveals some significant characteristics of the runoff schemes.

First, the ECMWF runoff is much smoother than the results predicted by the HBV-scheme. Surface runoff, occurring after heavy precipitation or snow melt events, is simulated at only few occasions, such as during an extremely heavy precipitation event on 15 July, giving a small peak of the runoff curve. All remaining days, the runoff originates solely from the deep-water drainage. Moreover, the ECMWF curve shows a general delay of the major runoff events compared to the HBV-output. This reflects the significant differences in the way the models treat the runoff process.

The ECHAM4 scheme follows the peaks in the HBV-output reasonably. The extremes early in the simulation period are higher than in the HBV-simulation. As a result, the dry-down period is likely to be reached a bit earlier. However, runoff during the first days is sensitive to the soil moisture initialization,

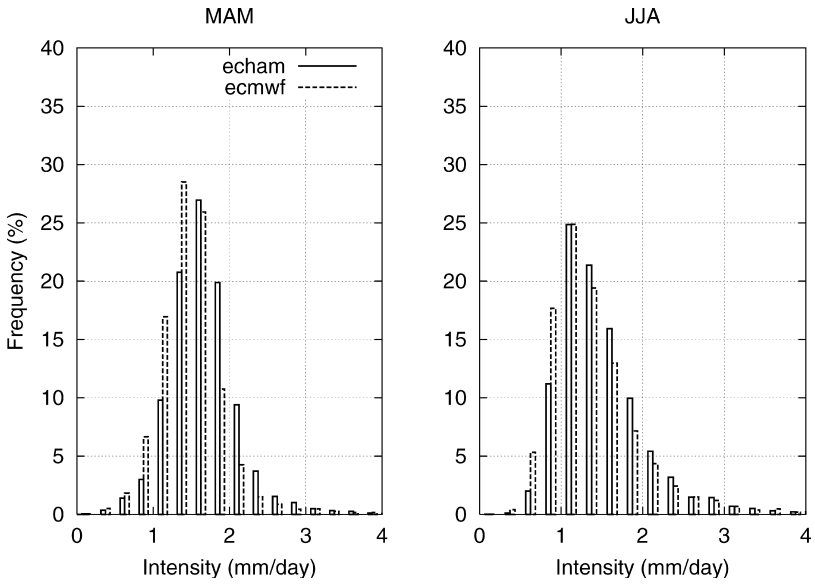

Fig. 6. Frequency distribution of number of RACMO gridpoints with indicated average total precipitation (mm/day) using the ECHAM4 and ECMWF surface schemes, separately for the periods March–April–May (left) and June–July–August (right).

since the runoff generation in this range is very efficient. An initialization to field capacity (75% of W_{sat}) rather than at saturation would have reduced the runoff in the first month by approximately 75% (results not shown).

The frequency distribution of the runoff results in Fig. 7 are shown in Fig. 8. Only runoff calculations in the period 1 April–31 October are considered in the frequency distribution. The ECMWF scheme does not simulate very low (<0.25 mm/day) runoff intensities, in contrast to HBV and ECHAM4. Differences in the potential infiltration (liquid precipitation + snow melt) cannot explain this different behaviour of ECMWF, since the RACMO model with ECMWF has a stronger preference in generating low potential infiltration rates, similar to the precipitation frequency distribution shown in Fig. 6. Similarly, high runoff intensities are also rare in ECMWF. The results from ECHAM4 and HBV are rather similar, showing more frequent occurrences of both low and high runoff intensities. In both models, runoff has a unimodal distribution, but the tail of high runoff intensities (>3 mm/day, shown as a single bar in Fig. 8) in the ECHAM4 scheme appears more dominant than in HBV. HBV and ECHAM4 runoff production is more strongly correlated to the potential infiltration than ECMWF.

The spatial distribution of the runoff over the catchment area is significantly different for the ECMWF and ECHAM4 schemes. In Fig. 9, the relative runoff is plotted, defined as the total runoff divided by the potential infiltration in the period April–October 1995. High values are found in the North-Scandinavian mountain area. In general, the ECMWF relative runoff exhibits a much smoother pattern than the ECHAM4 distribution. The latter produces little runoff in the flat area in Germany and Poland, while more runoff is produced in the mountainous high latitude subbasins in the catchment.

Fig. 10 shows the dependence of relative runoff on the orographic standard deviation σ_o (see Eq. (2)) for both the ECMWF and ECHAM4 scheme. Shown is the normalized relative runoff, which is for each RACMO grid box i calculated from the accumulated runoff R_i and throughfall T_i, normalized by the model dependent catchment average runoff $\bar{R}$ and throughfall $\bar{T}$ as

$$\frac{R_i}{T_i}\frac{\bar{T}}{\bar{R}}. \tag{11}$$

This normalization filters out the effect of both orography and model formulation on the precipitation driving the runoff. It can clearly be seen that

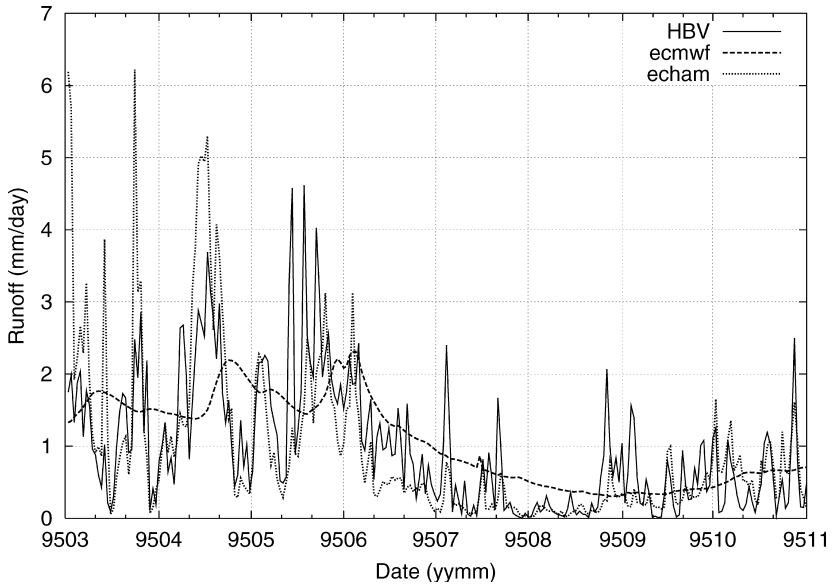

Fig. 7. Runoff to the Baltic Sea as calculated from HBV-Baltic and from the RACMO atmospheric model with the ECHAM4 and ECMWF land surface schemes. Shown are daily totals for all land area in the catchment.

ECHAM4 exhibits a greater sensitivity of runoff to orographic variance than ECMWF. However, the ECMWF runoff scheme also shows a pronounced sensitivity to orography. This is caused by the fact that more precipitation in mountainous areas results in a higher soil moisture content, which drives the runoff process via Eq. (6).

Apart from orographic variability, spatial variation

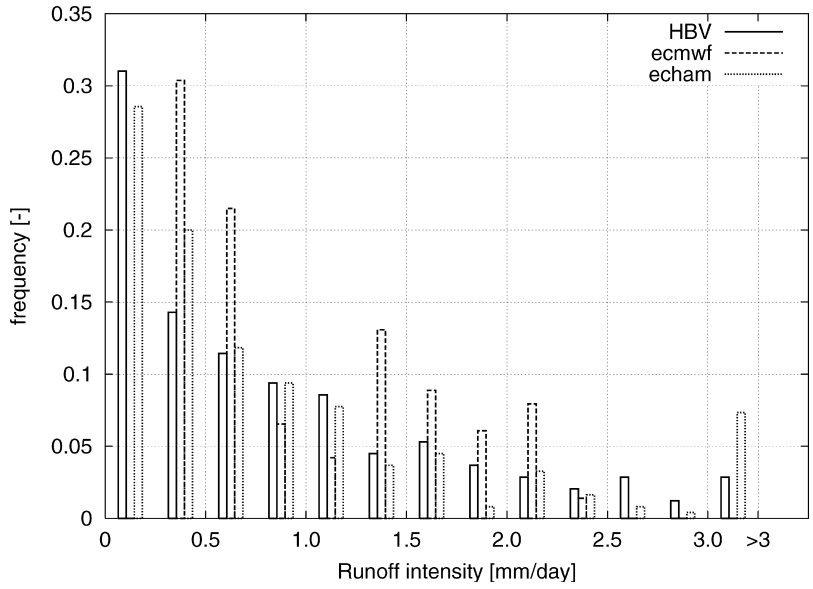

Fig. 8. Frequency distribution of daily runoff generation for the models shown in Fig. 7. Calculations are based on daily catchment averaged totals between 1 April and 31 October 1995.

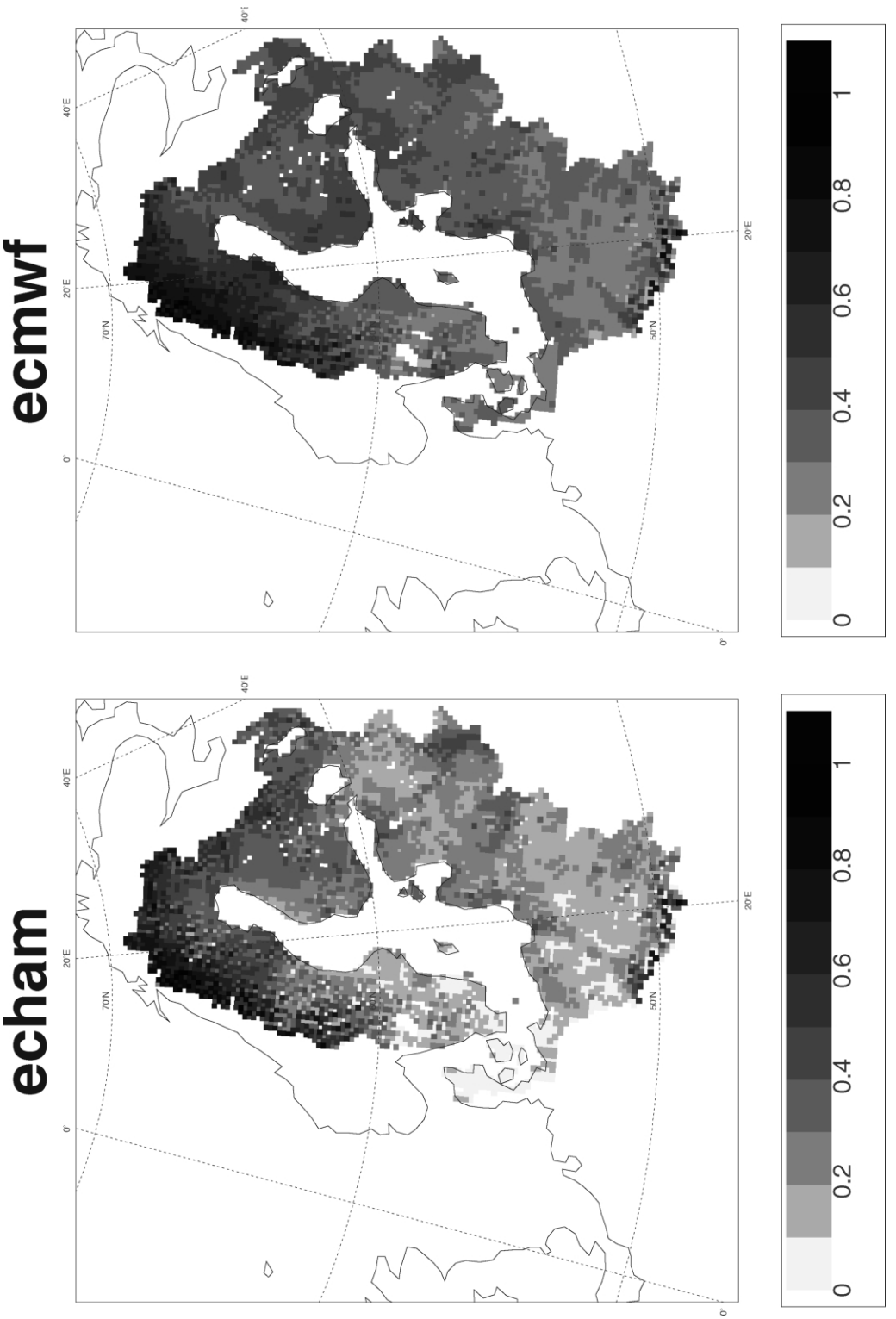

Fig. 9. Spatial distribution of relative runoff (runoff divided by total precipitation minus snowfall plus snowmelt), accumulated over the period 1 April–31 October 1995, for the ECHAM4 scheme (left) and ECMWF scheme (right).

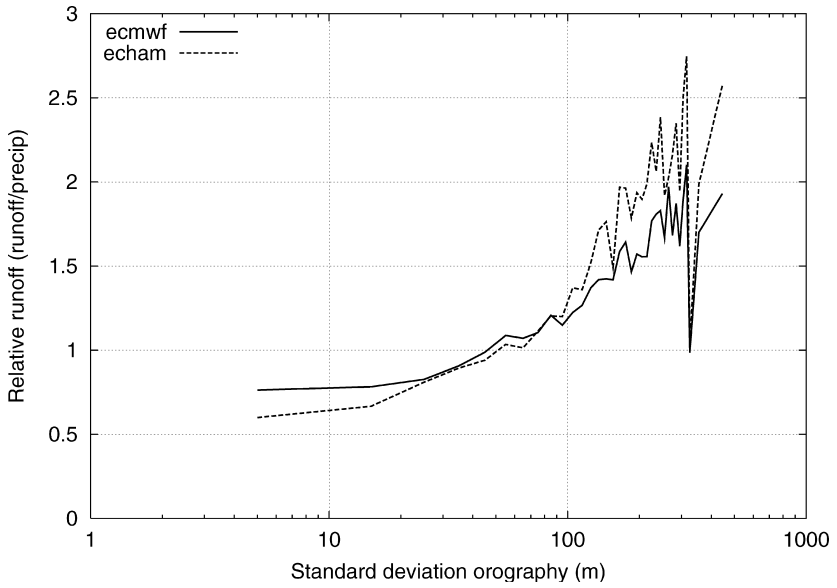

Fig. 10. Normalized relative runoff $(R_i/T_i)\ R_i/T_i(\bar{T}/\bar{R})$ plotted as function of orographic standard deviation σ_o from the sample of catchment grid boxes, calculated from the April–October totals using both ECHAM4 and ECMWF surface schemes.

of runoff is also caused by a variability in maximum water holding capacity in the soil and the dynamics of the snow pack. We have analysed separately HBV-Baltic and RACMO model results for two distinct hydrological catchments (see Fig. 2). The catchments are different with respect to the terrain height variability (mountainous in the Bothnian Bay catchment, flat near the Gulf of Riga), water holding capacity (shallow in the mountain area, deeper in the flat basin) and the snow dynamics (deep winter snow pack in the Northern catchment, little snow in the Eastern).

Fig. 11 shows the relation between relative runoff and catchment root zone soil water deficit, for each model version and for the total Baltic catchment as well as the two subbasins. In HBV, the non-linearity in this relation (Fig. 3) causes a slightly weaker slope for the entire catchment than for the individual subbasins. The smaller range in soil water deficit in the Bothnian Bay catchment (associated with a smaller water holding capacity) is responsible for a high runoff intensity. For ECHAM4, the runoff generation falls significantly steeper with increasing soil water deficit, which is the background of the small runoff intensities in the flatter areas shown in Fig. 9.

For the ECMWF model, the dependence of runoff intensity on root zone soil water deficit is much less pronounced. The slow response of runoff to potential infiltration is caused by the fact that high frequency oscillations in the forcing can effectively be smoothed by additional diffusion of water within the soil before the infiltrated water leaves the soil volume as deep drainage. Viterbo and Beljaars (1995) analysed the time scales of the ECMWF soil hydraulic parameterization for wetness conditions up to field capacity. Their analysis shows that several months are required to obtain a response of soil water in the deepest layer to surface forcings. In this study, however, the strongest events take place at even wetter soils (or rapidly cause the upper soil layer to become nearly saturated), which acts to decrease the time scales of the soil hydraulic processes significantly.[1]

An analysis of the correlation between infiltration events and runoff generation for the Bothnian Bay subcatchment reveals an undelayed runoff response for the ECHAM4 and HBV simulations. In the ECMWF scheme, the marked potential infiltration associated with the spring snow melt in this subcatchment is

[1] At field saturation, the hydraulic conductivity γ equals ± 0.39 m/day (see Table 2). If the whole column would be at or close to saturation, this implies that 3.5 days are required to drain the water through a 1.36 m deep water volume.

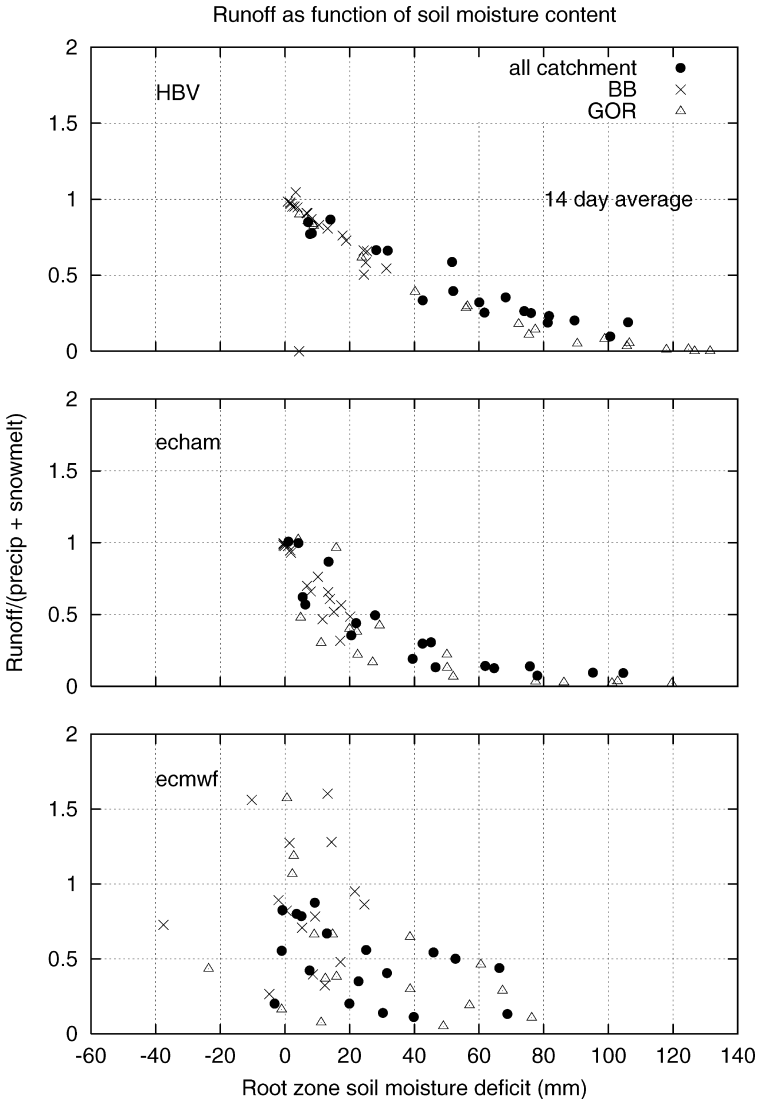

Fig. 11. Runoff divided by potential infiltration (precipitation + snow melt) as function of catchment soil water deficit for the HBV model (top), ECHAM4 (centre) and ECMWF (bottom). Shown are 14-day averages for the total Baltic catchment, as well as for the smaller subcatchments discharging to the Bothnian Bay (BB) and to the Gulf of Riga (GOR).

seen in the runoff signal with a clear delay. The maximum correlation between potential infiltration and runoff occurs after approximately 8 days in this mountainous subbasin. In the flat basin of the Gulf of Riga, a major infiltration similar to the spring snow melt is not present. In the ECMWF scheme, no significant correlation between daily runoff and daily infiltration was observed, while ECHAM4 and HBV show a high correlation only when no time delay is applied to the runoff time series (figures not shown).

4.3. Seasonal cycle of the land surface hydrology

The impact of the land surface parameterizations on the water budget at monthly or seasonal time scales is shown in Fig. 12, where land hydrology budgets for the period between 1 April and 31 October are shown.

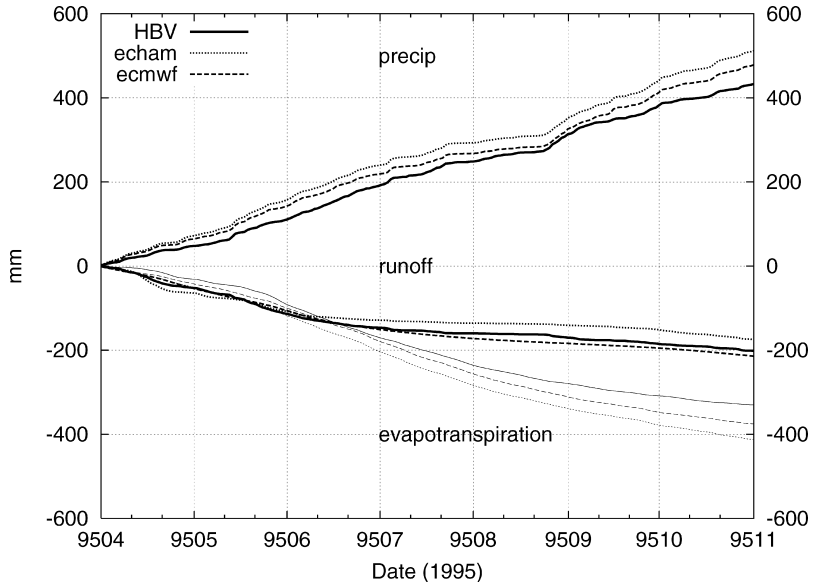

Fig. 12. Cumulative precipitation (positive), total runoff and evapotranspiration (both negative) in the period April–October 1995 for HBV-Baltic, ECMWF and ECHAM4. The HBV-Baltic precipitation (from synoptic stations) includes corrections for aerodynamically induced undercatch.

Precipitation is plotted as positive values, and both runoff and evapotranspiration are shown negative. In spring, ECHAM4 produces more runoff than any of the other schemes. On the other hand, accumulated over the total 7-month period, ECHAM4 gives 28 mm less runoff than the HBV total (which is 202 mm). ECMWF corresponds well to HBV, generating only 12 mm more runoff.

The smaller ECHAM4 runoff in the accumulation period is remarkable, given the rather large differences in total precipitation for the period. The HBV synoptic dataset results in a total accumulated precipitation of 433 mm, which is exceeded by ECMWF by 45 mm and by ECHAM4 by 79 mm. The HBV dataset may be biased a bit low, in particular early in the period when snow fall occurs. The ratio of total runoff to total precipitation in the ECMWF LSP is at 45% very close to the estimation in HBV (47%). In ECHAM4, this relative runoff is much lower (34%).

The total land surface evapotranspiration in ECHAM4 is 37 mm higher than in ECMWF, in spite of the considerable reduction (77 mm) of the infiltration due to the high surface runoff generation. The higher infiltration is mainly compensated by a reduced bottom drainage (keeping more water in the soil available for evapotranspiration). This causes a smaller depletion of the soil moisture reservoir and reduces the soil moisture stress on canopy transpiration.

Estimations of the surface evaporation on the regional scale of the catchment were not available. Instead, model computed relative humidity at screen level (2 m) height was compared to operational synops observations in the area (Fig. 13). Relative humidity is a quantity only indirectly related to surface evaporation, but its dependence on both air temperature and air humidity combines the effects of air humidity and available energy on the surface evaporation. The weekly averaged relative humidity scores clearly show a high bias in the early season for both surface schemes, and a dry bias in the summer months, which is stronger in the ECMWF scheme. The high bias in the winter/spring season is barely related to the soil hydrology in the models, but more so to evaporation of interception and snow (Beljaars and Viterbo, 1994; Van den Hurk et al., 2001). In the growing season starting in, say, May, the soil hydrology is more strongly correlated to the surface evaporation; the relative humidity data suggest an

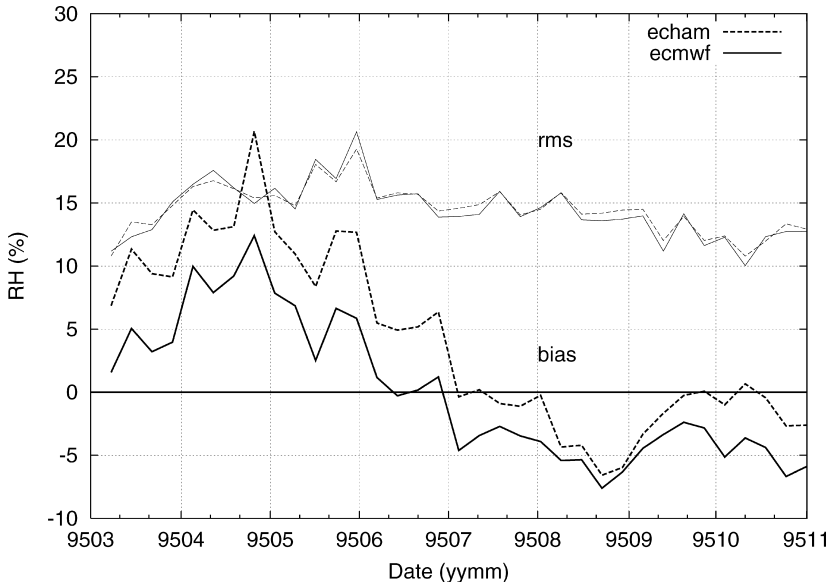

Fig. 13. Bias (thick lines) and root mean square error (corrected for bias) (thin lines) of near surface relative humidity in the catchment area for RACMO with the ECHAM4 and ECMWF surface schemes. Shown are 7-day averages of comparisons to observations from approximately 250 synops stations in the catchment area.

underestimation of the evaporation of the ECMWF scheme for the whole summer.

5. Summary and discussions

In this paper, we have analysed simulations of runoff and soil hydrological budgets from the Baltic Sea catchment area using two different LSP schemes embedded in a common regional climate model. The runoff simulations were compared to calculations of a calibrated large-scale hydrological model of the area, HBV-Baltic.

The runoff parameterizations discussed here may be considered to represent two generally different approaches in the simulation of large-scale runoff. In the ECHAM4 scheme, runoff occurs when precipitation and/or melting snow is provided to a model grid box which is assumed to be partially saturated with soil water. The relative saturation of the grid box is a parameterized function of average water content and orographic variability. In the ECMWF surface scheme, runoff is the result of a free drainage bottom boundary condition, where the free drainage rate is calibrated on an 'average' soil texture.

The scheme of Dümenil and Todini (1992) was originally designed for application at the global scale at T21 resolution (approximately $1000 \times 1000\ \mathrm{km}^2$). After tuning of $\sigma_{\min}$ and $\sigma_{\max}$, it has been applied at T106. Although it is not designed for application at a spatial resolution as used in this study (approximately $18 \times 18\ \mathrm{km}^2$) without additional recalibration of the orographic coefficients, this has been applied in regional climate models before (e.g. Jacob and Podzun, 1997). Similarly, the use of the Richards equation, which is the basis of the land surface scheme of (Eq. (5)) is a physically comprehensible parameterization in terms of the interaction between moisture content and hydraulic properties, but is rather unrealistic at the scale of operation. Both parameterizations must therefore be considered as a pragmatic solution to the very complex problem of soil hydrological spatial heterogeneity and temporal characteristics.

Both the temporal and spatial runoff patterns, considered during simulations spanning a period of 8 months covering the 1995 growing season, appear to be rather different. The ECHAM4 variable infiltration approach exhibits strong temporal fluctuations at short time scales, and the frequency distribution of runoff

events resembles the HBV calculations rather well. In contrast, the approach followed in the ECMWF surface scheme filters the (potential) infiltration signal before draining the water through the lowest boundary, and displays a delayed runoff response to major infiltration events.

Also, spatial patterns are quite different. To some extent, ECMWF is able to capture regional differences in the relative runoff (R/T) as a result of local differences in the precipitation, evaporation and soil moisture content averaged over the period. On the other hand, the variability of R/T is small compared to ECHAM4. It does not include an explicit dependence of runoff on orographic variability and soil water deficit. Such dependence in the ECHAM4 scheme enhances spatial patterns of high runoff rates in mountainous areas.

The hydrological budgets for the simulation period (discarding the first month) show remarkable differences between the schemes. While ECHAM4 produces higher runoff peaks and stronger short-term variability, the accumulated runoff is considerably lower than in the ECMWF and HBV schemes. As a result, more water is available for evaporation, which seems to feed back on the accumulated precipitation, which is also higher in the ECHAM4 version. In spite of the limited scope of these results, due to the limited timeframe of the intercomparison and additional subtle differences between the evaporation schemes of ECHAM4 and ECMWF, they show a strong indication of the impact of the runoff parameterization on the hydrological cycle in a large area.

In the new version of the ECMWF LSP (Van den Hurk et al., 2001), the treatment of the soil hydrology remains unchanged in unfrozen soils. However, a revision of the runoff treatment, the implementation of variable soil types, and a different formulation of the hydrological coefficients is the subject of ongoing research. Including detailed hydrological knowledge and river discharge data as done in this study would provide valuable guidance for these future developments. For instance, in the context of a PILPS2E project, various versions of the new ECMWF scheme are compared in an offline experiment focusing on the hydrology in a catchment close to the Bothnian Bay subcatchment addressed in this study (Lettenmaier and Bowling, 2000). Preliminary results show a beneficial impact on the timing and frequency distribution of the catchment scale runoff when a variable infiltration capacity scheme is used to simulate surface runoff in the ECMWF model.

The strategy to execute two isolated simulations only differing with respect to the land surface scheme enables to focus on the effect of these model components. However, it is not able to distinguish the signal arising from the land component change from the atmospheric noise inherent in seasonal simulations. To evaluate the significance of the model changes, the differences should be compared to standard deviations generated in an ensemble of model simulations (see e.g. Koster et al., 2000), but this was not carried out in the present study.

6. Conclusions

From the study described in this paper, several conclusions can be drawn. First, the ECHAM4 land surface scheme shows runoff results that agree well with established hydrological modelling experience. The deficiencies in this approach could benefit from additional study of the orographical relationship in the parameterization.

Second, the ECMWF parameterization appears to suffer from both an excessive time filtering of the runoff generation components, and a disregard of the important relationship between soil moisture content and runoff generation. A revision of the soil hydraulic equations and the inclusion of geographical heterogeneity of these would likely lead to better runoff predictions.

Third, the use of a common regional atmospheric host model coupled to different land surface parameterization schemes enabled demonstration of the effect of the LSP on the hydrological cycle on the scale of a large catchment. The seasonality of runoff generation affects soil water storage and thus evapotranspiration in a later stage. The strong coupling between local evapotranspiration and local precipitation in this area results in clear hydrological feedback mechanisms.

Acknowledgements

Daniela Jacob and Lennart Bengtsson have taken an important leading role in the NewBaltic2 EU project. Sten Bergström and Anton Beljaars have

provided many encouraging and constructive discussions and suggestions. Erik van Meijgaard assisted considerably with the operation of RACMO. Bert Holtslag supervised the KNMI-contribution to NewBaltic2. Also, two anonymous reviewers provided many useful comments. This work is partially sponsored by the EU under contract number ENV4-CT97-0626, and the national research program NRSP-2 under contract number 951246.

Appendix A. Additional parameterizations in the ECHAM4 scheme

In the ECHAM4 scheme, precipitation P and snow melt M may be (partially) intercepted by vegetation canopies. The net input to the soil reservoir consists of the througfall T, given by:

$$T = (P + M - I) \tag{A1}$$

with interception I given by:

$$I = \min\left(c_I k_I P, \frac{W_{\mathrm{lmx}} - W_{\mathrm{l}}}{\rho_{\mathrm{w}} \Delta t}\right) \tag{A2}$$

c_I is an interception efficiency and equal to 1, and k_I, a precipitation heterogeneity coefficient, equal to 1 for both large scale and convective precipitation. W_{lmx} is the maximum interception layer depth (2 mm per unit leaf plus soil area), W_{l} the actual interception layer depth, ρ_{w} the water density and Δ_{t}, the time step length. Melted snow is first accumulated in the interception layer, and put in throughfall when $W_{\mathrm{l}} \geq W_{\mathrm{lmx}}$.

The formulation of surface evaporation is based on an earlier version of the ECMWF surface scheme (Blondin, 1991). Surface evaporation is a combination of evaporation from the interception layer, from the snow deck, from the bare ground area in the grid box, and from the vegetation. Interception evaporation E_I, is at the potential rate, calculated as (defined positive downward)

$$E_I = \rho_{\mathrm{a}} |U_{\mathrm{a}}| C_{\mathrm{H}} (q_{\mathrm{a}} - q_{\mathrm{sat}}(T_{\mathrm{s}})), \tag{A3}$$

with ρ_{a}, the air density, U_{a}, the wind speed at the lowest model level, C_{H}, the bulk transfer coefficient for heat and moisture, q_{a}, the specific humidity at the reference level, and $q_{\mathrm{sat}}(T_{\mathrm{s}})$, the saturated specific humidity at surface temperature T_{s}. Snow evaporation E_{s} is calculated identically to E_I. Bare ground evaporation E_{b} is similar to Eq. (A3), apart from the parameterization of a relative humidity at the soil surface, α_{h}:

$$E_{\mathrm{b}} = \rho_{\mathrm{a}} |U_{\mathrm{a}}| C_{\mathrm{H}} (q_{\mathrm{a}} - \alpha_{\mathrm{h}} q_{\mathrm{sat}}(T_{\mathrm{s}})). \tag{A4}$$

In ECHAM4, α_{h} is parameterized as

$$\alpha_{\mathrm{h}} = 0.5\left[1 - \cos\left(\pi \frac{(W - W_{\mathrm{sat}} + W_{\mathrm{b}})}{W_{\mathrm{b}}}\right)\right], \tag{A5}$$

with W_{b} a bare soil evaporation threshold:

$$W_{\mathrm{b}} = \min(W_{\mathrm{sat}}, 0.1). \tag{A6}$$

Canopy evaporation E_{v} uses an additional canopy resistance r_{c}, according to:

$$E_{\mathrm{v}} = \frac{\rho_{\mathrm{a}}}{r_{\mathrm{c}} + (|U_{\mathrm{a}}| C_{\mathrm{H}})^{-1}} (q_{\mathrm{a}} - q_{\mathrm{sat}}(T_{\mathrm{s}})). \tag{A7}$$

r_{c} is a function of absorbed photosynthetic active radiation (PAR), leaf area index L, soil moisture content and a minimum stomatal resistance $r_{\mathrm{s,min}}$, following:

$$r_{\mathrm{c}} = \frac{r_{\mathrm{s,min}}}{L} f_1(\mathrm{PAR}) f_2(W). \tag{A8}$$

f_1 is equal to the analytical expression for light absorption in a canopy with horizontal leaves, derived by Sellers (1985). PAR is assumed to be 55% of the net shortwave radiation. f_2 is a linear stress function, formulated as:

$$f_2(W) = \begin{cases} 0 & W < W_{\mathrm{pwp}} \\ \dfrac{W - W_{\mathrm{pwp}}}{W_{\mathrm{cap}} - W_{\mathrm{pwp}}} & W_{\mathrm{pwp}} \leq W \leq W_{\mathrm{cap}} \\ 1 & W > W_{\mathrm{cap}} \end{cases}, \tag{A9}$$

where $W_{\mathrm{pwp}} \equiv 0.35 W_{\mathrm{sat}}$ is assumed to be the soil wilting point, and $W_{\mathrm{cap}} \equiv 0.75 W_{\mathrm{sat}}$ is the field capacity.

$r_{\mathrm{s,min}}$ in Eq. (A8) is 100 s/m everywhere in the domain. The leaf area index varies with location (Claussen et al., 1994) but is kept constant throughout the season.

In the ECHAM4 scheme, the surface energy balance equation is solved for the entire grid box as a whole, yielding a single grid box surface temperature. The net fluxes between the surface and the atmosphere are dependent on the relative areas of each of the subcomponents of the land surface: the snow deck, the bare soil part, the vegetation part and the interception layer. The temperature of the upper soil layer of

depth 6.5 cm is the surface temperature used in the computation of turbulent heat fluxes.

Appendix B. Additional parameterizations in the ECMWF scheme

In contrast to the ECHAM4 scheme, the surface temperature in ECWMF is a skin temperature, calculated for a layer without heat capacity between the soil and the atmosphere. It reacts quickly to changes in radiative and turbulent forcings, and damps the diurnal cycle of the soil heat flux.

The formulation of evaporation from the snow deck, interception reservoir, bare soil and vegetation follows the same procedures as in ECHAM4. There are some differences in parameter choices, which have consequences for the calculated evaporation rates. The bare ground evaporation is calculated similar to 15, but α_h is formulated somewhat differently:

$$\alpha_h = 0.5\left[1 - \cos\left(1.6\pi \frac{w_1 - w_{pwp}}{w_{cap} - w_{pwp}}\right)\right], \qquad \text{(B1)}$$

where now the soil moisture content of the top layer is used. The factor 1.6 is added to mimic the moisture difference between the bulk of the top layer and the level just below the surface.

For the simulations shown, the original constant leaf area index of 4 m^2/m^2 is replaced by a geographically variable value. Also, the default value of $r_{s,min}$ was set at 100 rather than 240 s/m, while the ratio of PAR to total shortwave radiation is 55% rather than 50%, to increase compatibility to ECHAM4. Remaining differences compared to ECHAM4 are:

- The roughness length for heat, determining the aerodynamic transfer coefficients for heat and moisture, is 0.1 × the momentum roughness length. In ECHAM4, these two roughness lengths are identical.
- The interception efficiency c_I (Eq. (A2)) is 0.5, while $k_I = 1$ for large scale and 2 for convective precipitation, respectively. Thus, large-scale interception is half the ECHAM4 value, while convective interception is identical.
- Water is extracted from the top three layers rather than from a single bucket. The roots are distributed equally over the three layers, which, as the layers increase approximately exponentially with depth, result in an approximately exponential extraction profile.
- The soil moisture stress term for r_c (Eq. (A9)) is expressed in terms of a weighted average soil moisture content in the root zone. The weighing of each layer is according to relative root extraction from that layer.

These differences have as net result that for a given radiative forcing and soil moisture content, the ECMWF canopy resistance is approximately 40% higher than in the ECHAM4 scheme. Since evaporation is not solely determined by the canopy resistance, the difference in total evaporation is less.

References

Beljaars, A.C.M., Viterbo, P., 1994. The sensitivity of winter evaporation to the formulation of aerodynamic resistance in the ECMWF model. Bound. Layer Meteorol. 71, 135–149.

Bergström, S., 1995. The HBV model. In: Singh, V.P. (Ed.). Computer Models of Watershed Hydrology. Water Resources Publication, Highlands Ranch, Colorade, pp. 443–476.

Bergström, S., Forsman, A., 1973. Development of a conceptual deterministic rainfall–runoff model. Nordic Hydrol. 4, 147–170.

Bergström, S., Graham, L.P., 1998. On the scale problem in hydrological modelling. J. Hydrol. 211, 253–265.

Betts, A.K., Viterbo, P., 2000. Hydrological budget and surface energy balance of seven sub-basins of the Mackenzie River from the ECMWF model. J. Hydrometeorol. 1, 47–60.

Betts, A.K., Viterbo, P., Wood, E.F., 1998. Surface energy and water balance for the Arkansas-Red river basin from the ECMWF reanalysis. J. Climate 11, 2881–2897.

Betts, A.K., Ball, J.H., Viterbo, P., 1999. Basin-scale surface water and energy budgets for the Mississippi from the ECMWF reanalysis. J. Geophys. Res. 104D, 19293–19306.

Blondin, C., 1991. Parameterization of land surface processes in numerical weather prediction. In: Schmugge, T.J., André, J.C. (Eds.). Land Surface Evaporation: Measurements and Parameterization. Springer, Berlin, pp. 31–54.

Carlsson, B., 2000. Hydrological Data Centre for BALTEX (BALTEX HDC) — Status Report. Swedish Meteorological and Hydrological Institute, Norrköping, Sweden 49pp.

Christensen, J.H., Christensen, O.B., Lopez, P., van Meijgaard, E., Botzet, M., 1996. The HIRHAM4 regional atmospheric climate model. , Scientific Report 96-4. Danish Meteorological Institute, Copenhagen 51pp.

Clapp, R.B., Hornberger, G.M., 1978. Empirical equations for some hydraulical properties. Water Resour. Res. 14, 601–604.

Claussen, M., Lohmann, U., Roeckner, E., Schulzweida, U., 1994.

A Global Dataset of Land-Surface Parameters. Max-Planck-Institut fur Meteorologie, Hamburg 23pp.

Desborough, C.E., 1999. Surface energy balance complexity in GCM land surface models. Climate Dyn. 15, 389–403.

Dickinson, R.E., Henderson-Sellers, A., Kennedy, P.J., 1993. Biosphere–Atmosphere Transfer Scheme (BATS) for the NCAR Community Climate model. NCAR Technical Note NCAR/TN-275 + STR, 72pp.

Dirmeyer, P., Dolman, A.J., 1998. Gewex soil wetness project: preliminary report on the pilot phase. , IGPO Publication Series 29. IGO 48pp.

Dümenil, L., Todini, E., 1992. A rainfall–runoff scheme for use in the Hamburg climate model. In: O'Kane, J.P. (Ed.). Advances in Theoretical Hydrology. European Geophysical Society, Series on Hydrological Sciences, vol. 1. Elsevier, Amsterdam, pp. 129–157.

Gates, W.L., 1992. AMIP: the atmospheric model intercomparison project. Bull. Am. Meteorol. Soc. 73, 1962–1970.

Gibson, J.K., Kallberg, P., Uppala, S., Hernandez, A., Nomura, A., Serrano, E., 1997. ERA description. , ECMWF Re-Analysis Project Report Series 1. ECMWF, Reading RG2 9AX, UK 72pp.

Giorgi, F., Marinucci, M.R., Bates, G.T., 1993. Development of a second-generation climate model (RegCM2). Part II. Convective processes and assimilation of lateral boundary conditions. Monthly Weather Rev. 121, 2814–2832.

Graham, L.P., 1999. Modelling runoff to the Baltic Sea. Ambio 28, 328–334.

Graham, L.P., Bergström, S., 2000. Land surface modelling in hydrology and meteorology — lessons learned from the Baltic Basin. Hydrol. Earth Sys. Sci. 4, 13–22.

Graham, L.P., Jacob, D., 2000. Using large-scale hydrologic modeling to review runoff generation processes in GCM climate models. Meteorol. Z. 9, 49–57.

Gustafsson, N., 1993. Hirlam 2 final report. Available from SMHI, S-60176 Norrköping, Sweden.

Hagemann, S., Dümenil, L., 1999. Application of a global discharge model to atmospheric model simulations in the Baltex region. Nordic Hydrol. 30, 209–230.

Hagemann, S., Dümenil, L., 2001. Validation of the hydrological cycle of ECMWF and NCEP reanalyses using the MPI hydrological discharge model. J. Geophys. Res. 106, 1503–1510.

Henderson-Sellers, A., Yang, Z.-L., Dickinson, R.E., 1993. The project for intercomparison of land-surface intercomparison schemes. Bull. Am. Meteorol. Soc. 74, 1335–1349.

Jacob, D., Podzun, R., 1997. Sensitivity studies with the regional climate model Remo. Meteorol. Atmos. Phys. 63, 119–129.

Jacob, D., van den Hurk, B.J.J.M., Andr, U., Elgered, G., Fortelius, C., Graham, L.P., Jackson, S.D., Karstens, U., Kpken, Chr., Lindau, R., Podzun, R., Rockel, B., Rubel, F., Sass, B.H., Smith, R.N.B., Yang, X., 2001. A comprehensive model intercomparison study investigating the water budget during the BALTEX-PIDCAP period. Meteorol. Atmos. Phys. 77, 19–44.

Koster, R.D., Milly, P.C.D., 1997. The interplay between transpiration and runoff formulations in land surface schemes used with atmospheric models. J. Climate 10, 1578–1591.

Koster, R.D., Suarez, M.J., Heiser, M., 2000. Variance and predictability of precipitation at seasonal-to-interannual timescales. J. Hydrometeorol. 1, 26–46.

Lau, K.-M., Kim, J.H., Sud, Y., 1996. Intercomparison of hydrologic processes in AMIP GCMs. Bull. Am. Meteorol. Soc. 77, 2209–2227.

Lettenmaier, D.P., Bowling, L., 2000. Arctic model intercomparison study initiated. GEWEX News WCRP 10, 8–10.

Liang, X., Wood, E.F., Lettenmaier, D.P., 1996. Surface soil moisture parameterization of the VIC-2L model: evaluation and modification. Glob. Planet. Change 13, 195–206.

Lindström, G., Johansson, B., Persson, M., Gardelin, M., Bergström, S., 1997. Development and test of the distributed HBV-96 hydrological model. J. Hydrol. 201, 272–288.

Liston, G.E., Sud, Y.C., Wood, E., Evaluating, G.C.M., 1994. Land surface hydrology by computing river discharges using a runoff routing model: application to the Mississippi basin. J. Appl. Meteorol. 33, 394–405.

Lohmann, D., Lettenmaier, D.P., Liang, X., Wood, E.F., Boone, A., Chang, S., Chen, F., Dai, Y., Desborough, C., Dickinson, R.E., Duan, Q., Ek, M., Gusev, Y.M., Habets, F., Irannejad, P., Koster, R., Mitchell, K.E., Nasonova, O.N., Noilhan, J., Schaake, J., Schlosser, A., Shao, Y., Shmakin, A.B., Versghy, D., Warrach, K., Wetzel, P., Xue, Y., Yang, Z.-L., Zeng, Q., 1998. The project for intercomparison of land-surface parameterization schemes (PILPS) phase 2(c) Red-Arkansas river basin experiment. 3. Spatial and temporal analysis of water fluxes. Glob. Planet. Change 19, 161–179.

Nash, J.E., Sutcliffe, J.V., 1970. River flow forecasting through conceptual models. Part I. A discussion of principles. J. Hydrol. 10, 282–290.

Noilhan, J., Mahfouf, J.-F., 1996. The ISBA land surface parametrisation scheme. Glob. Planet. Change 13, 145–159.

Omstedt, A., Mueller, L., Nyberg, L., 1997. Interannual, seasonal and regional variations of precipitation and evaporation over the Baltic Sea. Ambio 26, 484–492.

Pitman, A., Pielke, R., Avissar, R., Claussen, M., Gash, J., Dolman, H., 1999. The role of land surface in weather and climate: does the land surface matter?. IGBP Newslett. 39.

Robock, A., Schlosser, C.A., Vinnikov, K.Y., Speranskaya, N.A., Entin, J.K., Qiu, S., 1998. Evaluation of the AMIP soil moisture simulations. Glob. Planet. Sci. 19, 181–208.

Roeckner, E., Arpe, K., Bengtsson, L., Christoph, M., Claussen, M., Dümenil, L., Esch, M., Giorgetta, M., Schlese, U., Schulweida, U., 1996. The atmospheric general circulation model ECHAM4: model description and simulation of present-day climate. , Report No. 218. Max-Planck Institute für Meteorologie, Hamburg.

Sellers, P.J., 1985. Canopy reflectance, photosynthesis and transpiration. Int. J. Remote Sensing 6, 1335–1372.

Shao, Y., Anne, R.D., Henderson-Sellers, A., Irannejad, P., Thornton, P., Liang, X., Chen, T.H., Ciret, C., Desborough, C., Balachova, O., Haxeltine, A., Ducharne, A., 1994. Soil moisture simulation — a report of the RICE and PILPS workshop. , IGPO Publicaton Series No. 14. Clim. Impact Centre 179pp.

Van den Hurk, B.J.J.M., Viterbo, P., Beljaars, A.C.M., Betts, A.K.,

2001. Offline validation of the ERA40 surface scheme. ECMWF TechMemo 295.

Verseghy, D.L., 2000. The Canadian Land Surface Scheme (CLASS): its history and future. Atmosphere–Ocean 38, 1–13.

Viterbo, P., Beljaars, A.C.M., 1995. An improved land surface parametrization scheme in the ECMWF model and its validation. J. Climate 8, 2716–2748.

Viterbo, P., Courtier, P., 1995. The importance of soil water for medium-range weather forecasting. Implications for data assimilation. WMO Workshop on Imbalances of slowly Varying Components of Predictable Atmospheric Motions, Beijing, China, March 1995; WMO/TD 652, pp. 121–130.

Wetzel, P.J., Liang, X., Irannejad, P., Boone, A., Noilhan, J., Shao, Y., Kelly, C., Xue, Y., Yang, Z.L., 1996. Modeling vadose zone liquid water fluxes: infiltration, runoff, drainage interflow. Glob. Planet. Change 13, 57–71.

Wood, E.F., Lettenmaier, D.P., Liang, X., Lohmann, D., Boone, A., Chang, S., Chen, F., Dai, Y., Dickinson, R.E., Duan, Q., Ek, M., Gusev, Y.M., Habets, F., Irannejad, P., Koster, R., Mitchel, K.E., Nasonova, O.N., Noilhan, J., Schaake, J., Schlosser, A., Shao, Y., Shmakin, A.B., Verseghy, D., Warrach, K., Wetzel, P., Xue, Y., Yang, Z.-L., Zeng, Q.-C., 1998. The project for intercomparison of land-surface parameterization schemes (PILPS) phase 2(c) Red-Arkansas river basin experiment. 1. Experiment description and summary intercomparisons. Glob. Planet. Change 19, 115–135.